

Strong optical force induced by morphology dependent resonances

Jack Ng, C.T. Chan, and Ping Sheng

Department of Physics, Hong Kong University of Science and Technology, Clearwater Bay, Hong Kong, China

Zhifang Lin

Department of Physics, Fudan University, China

Compiled September 11, 2018

We consider the resonant optical force acting on a pair of transparent microspheres by the excitation of the Morphology Dependent Resonance (MDR). The bonding and anti-bonding modes of the MDR correspond to strong attractions and repulsions respectively. The dependence of the force on separation and the role of absorption are discussed. At resonance, the force can be enhanced by orders of magnitude so that it will dominate over other relevant forces. We find that a stable binding configuration can be induced by the resonant optical force.

Optical forces are useful in the manipulation of ultra-fine particles and mesoscopic systems, and the development is rather astounding in the last three decades. The most well known types of the optical forces are the radiation pressure and the optical gradient force. There is also an inter-particle optical force, induced by the multiple scattering of light.¹⁻⁷ We present here an interesting type of resonant inter-particle force. We will see that the tuning of the incident light frequency to the Morphology Dependent Resonance (MDR) of a cluster of transparent microspheres would induce a strong resonant optical force (MDR-force) between the spheres. The MDR of a pair of spheres had been observed in fluorescent^{8,9} and lasing¹⁰ experiments. Here we study theoretically the force induced by such resonances. We will see that the MDR-induced force, derived from the coherent coupling of the whispering gallery modes (WGM's), is a strong short ranged force that can be attractive or repulsive depending on whether the bonding mode (BM) or the anti-bonding mode (ABM) is excited. The strength of the optical forces can be enhanced by orders of magnitude when a MDR is excited. As microsphere cavities are emerging as an alternative to the photonic crystal in controlling light,⁸⁻¹⁰ the MDR-force may be deployed for the manipulation of a microsphere cluster.

In this paper, we calculate the electromagnetic (EM) forces acting on microspheres when WGM's or MDR's are excited. The optical force acting on a microsphere can be computed via a surface integral of the Maxwell stress tensor, \vec{T} , over the sphere's surface. The microspheres cannot respond to the high frequency component of the time varying optical force, so we calculate the time-averaged force $\langle \vec{F} \rangle = \oint \langle \vec{T} \rangle \cdot d\vec{S}$. The EM field required in evaluating \vec{T} is computed by the multiple scattering theory,^{1,11} which expands the fields in vector spherical harmonics. This formalism is quite possibly the most accurate method that can be applied. It is in principle exact, and the numerical convergence is being controlled by the maximum angular momentum (L_{max})

used in the expansion. The calculation for the resonance of dielectric microspheres near contact requires a high L_{max} ,¹² which is chosen so that further increase in L_{max} does not change the value of the calculated force. In most of the calculations, the size parameter (kR) is between 28 and 29, and $L_{max}=63$ was used. We adopt the Generalized Minimal Residual iterative solver (GMRES) for the linear system of equations.¹³ In the following, the WGM's will be labeled as “(l)TE(n)” or “(l)TM(n)”, where l and n are the mode and order number, and TE (TM) means transverse electric (magnetic) respectively. Unless otherwise noted, a linearly polarized incident plane wave with a modest intensity of 10^4 W/cm² is assumed throughout this paper. The spheres have radius $R=2.5$ μ m, with a dielectric constant $\epsilon=2.5281+10^{-4}i$. The loss level of $Im\{\epsilon\}=10^{-4}$ or smaller can be easily achieved with insulators, glass or possibly good quality polystyrene spheres.

The well-known WGM's for a transparent microsphere have many interesting properties and applications, mostly because of its high quality factor and the enhanced EM fields near the surface. While the fields can be enhanced by orders of magnitude when a WGM is excited, the radiation pressure is only increased by about 30% or less, as shown in Fig. 1(a). It is because the intensity distribution of a WGM is symmetrical, so that the gradient force acting on the sphere at any point is cancelled by its counterpart on the other side of the sphere. However, a much stronger enhancement in the optical force can be induced by the resonances involving two spheres. When two spheres are near each other, their EM modes are coherently coupled and split into BM's and ABM's through the quasi-normal mode splitting.^{5,12} The BM's (ABM's) have resonant frequencies that are lower (higher) than that of the single sphere, and have an even (odd) parity in the EM field distribution.¹² Unlike the single sphere resonance where the force is not enhanced that much, the MDR's correspond to strong attractions (BM's) or repulsions (ABM's) between the spheres. The overall intensity distribution of the two-

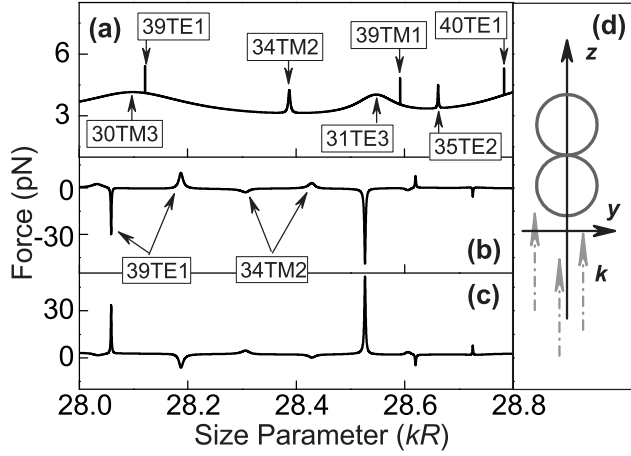


Fig. 1. (a): The radiation pressure for a sphere with $\varepsilon=2.5281$. (b)-(c): Optical forces acting on two contiguous microspheres ($\varepsilon=2.5281+10^{-4}i$), with configuration depicted in inset (d), with Panel (b) for the upper sphere and Panel (c) for the lower sphere. (d): A pair of contiguous spheres illuminated by a linearly polarized plane wave propagating along the bisphere (z) axis.

sphere resonance is still symmetrical, but the field pattern on each sphere is not. The strong internal fields then induce strong optical forces on the spheres. We note that the BM and ABM forces are also observed between layers of 2 dimensional photonic structure.⁵

In Fig. 1(b)-(c) we plot the optical forces acting on a pair of spheres with the geometry shown in Fig. 1(d). The wavelengths of the incident light fall inside the range of 542 nm to 561 nm, chosen to match with that of the previous works on MDR.^{12,14} The BM and ABM of 39TE1 and 34TM2 are marked on Fig. 1(b). When a resonance is excited, the force is tremendously enhanced compared to off-resonance. The BM's (ABM's) have the maximum (minimum) field intensity at the contact point of the spheres, giving rise to attractions (repulsions). The resonant linewidths of the MDR are also several orders of magnitude wider than that of a single sphere,^{12,14} and they are further broadened by absorption. We remark that the small peak at $kR=28.03$ in Fig. 1(b)-(c) is the ABM of 34TE2, and also the interactions between 39TM1 and 35TE2 complicated the splitting, and their coupling give rise to the MDR-force peaks at $kR=28.527$, 28.605 and 28.620.

One of the major challenges in studying MDR of spheres experimentally is that the resonant frequency is very sensitive to the size of the sphere and thus requires extremely accurate particle sizing.¹⁴ This difficulty has been overcome by utilizing the narrow linewidth of the single sphere resonance to determine the particle size.⁸⁻¹⁰ Nevertheless, the MDR force is actually quite robust against size dispersion. The solid line in Fig. 2 shows the MDR force at $kR=28.527$ when the two spheres are of the same diameter, to be compared with the forces in which the two spheres differ by 2% in diam-

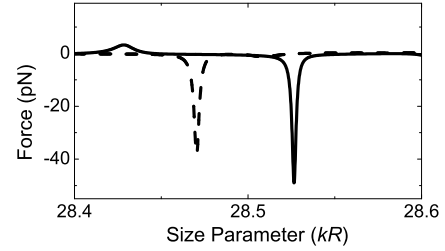


Fig. 2. Optical forces acting on a pair of spheres with the configuration shown in Fig. 1(d). The horizontal axis is the size parameter of the bottom sphere. Solid lines: both spheres have radius of $2.5 \mu\text{m}$. Dotted lines: The bottom sphere has radius of $2.5 \mu\text{m}$ and the top sphere has radius of $2.45 \mu\text{m}$.

eter (dotted line). We see that the MDR force remains significant even when the two spheres do not have the same radius.

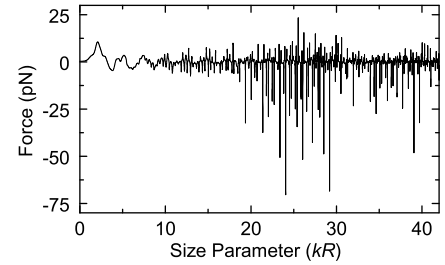


Fig. 3. Optical forces as a function of the size parameter acting on two contiguous spheres as depicted in Fig. 1(d). $\varepsilon=2.5281+10^{-4}i$. Only the force acting on top sphere is plotted.

Figure 3 shows the forces acting on a pair of spheres over a wide range of size parameters. From this figure, we see that the attractive resonant force is generally stronger than the repulsive resonant force. The resonant force is most significant for spheres with size parameters between 20 and 30. The force for those with size parameters greater than 30 is damped by absorption.

The MDR frequencies actually depend on the distance between the spheres, and this property can be utilized to bind the spheres into a stable structure. As an illustrative example, we consider a pair of spheres (aligned along z -axis) illuminated by an incident field of the form $\vec{E}_{in} = \hat{x}E_o \sin(kz)$, which compose of a pair of counter-propagating waves going along the bisphere axis. At a particular frequency of the incident wave, slightly higher than the resonant frequency of a WGM, the ABM is excited at a particular distance between the spheres, leading to strong repulsion. However, at distances larger than

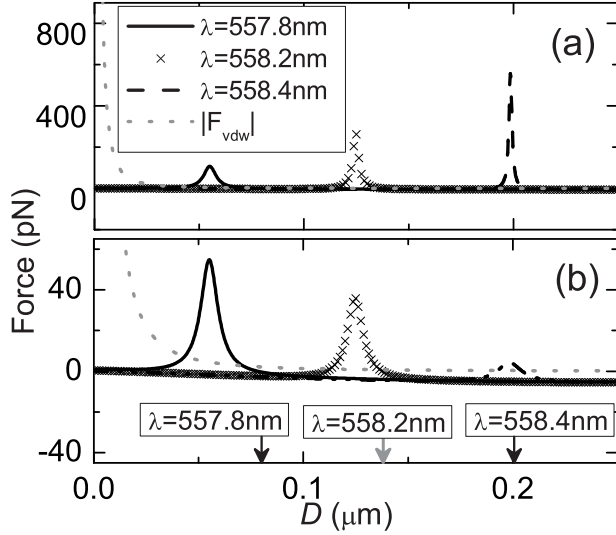


Fig. 4. Optical force acting on a pair of spheres plotted as a function of D , the separation between the closest points on the spheres. The forces acting on the spheres are equal and opposite by symmetry, with positive force represents repulsion and vice versa. The positions of the spheres are $(0, 0, -D/2 - R)$ and $(0, 0, D/2 + R)$. The incident wave has the form $\vec{E}_{in} = \hat{x}E_o \sin(kz)$. The 39TE1 resonance of a single sphere is at $\lambda=558.6$ nm. $|F_{vdw}|$ is an upper bound of the magnitude of the van der Waals force. (a): Ideal case with no absorption, i.e. $\varepsilon=2.5281$. (b) $\varepsilon=2.5281+10^{-4}i$. The stable equilibrium separations (optical force equals zero and stable against perturbation) for different incident wavelengths are marked by arrows.

that particular distance, both the radiation pressure and the Van der Waals forces will push the balls together. This competition between ABM resonant repulsion and other attractive forces lead to the stable position. Figure 4 shows the force as a function of D , the separation between the closest points on the spheres. The dielectric constant is taken to be $2.5281+10^{-4}i$ in Fig. 4(b), and the ideal case results with no absorption ($\varepsilon=2.5281$) are shown in Fig. 4(a) for comparison. Stable equilibrium separations, where the optical force is zero, are marked by arrows in Fig. 4(b). The spheres will experience an attractive (repulsive) force if their separation is increased (decreased) from the equilibrium distance. Binding can also be achieved by using two lasers, one tuned to a BM and the other tuned to an ABM such that there is an equilibrium separation “sandwiched” by the resonant force peaks. The interaction between the two laser beams can be neglected because of the lack of coherence.

We also compare the MDR-force with other relevant interactions. The energy associated with the repulsive barriers created by the ABM’s are on the order of tens of k_bT (the thermal energy at room temperature) at an incident intensity of 10^4 W/cm². For example, it takes

about $80 k_bT$ to push the spheres across the middle peak of Fig. 4(b) (corresponding to $\lambda=558.2$ nm). Another relevant comparison is the strength of the van der Waals forces. An upper bound on the magnitude of the van der Waals force between two dielectric spheres, $|F_{vdw}|$, can be calculated by the non-retarded approximation: $|F_{vdw}(D)| \leq AR/12D^2$, where $A=6.6 \times 10^{-20}$ Joule is the Hamaker constant.¹⁵ The magnitude of the van der Waals force is plotted on Fig. 4. One sees that the resonant force can dominate over the van der Waals force if the D is more than a few tens of nano-meter. Finally, the weight of a glass sphere (mass density = 2400 kg/m³) is about 1.5 pN.

We note from Fig. 4 that the resonant separation (where the force is maximum) increases as the incident frequency is tuned closer to the resonant frequency of the WGM. This can be understood from the fact that a larger separation corresponds to a smaller splitting of the WGM. In the ideal case with no absorption (see 4(a)), the strength of the MDR-force is an increasing function of resonant separation. This is because the quality factor, and thus the internal field of the MDR, attains the huge values of the WGM as the separation increases.¹² We note that resonant force for the ideal case approaches a nano-Newton. However, in reality the resonances are inevitably subject to absorptive losses.

We emphasize that the properties of the resonant mode is determined by the morphology. As long as the incident frequency matches the resonant frequency, the resonance will be excited irrespective of the external light profile. However, it is the projection (coupling) of the incident light onto the resonating mode that determines the strength of the resonant force. A plane wave is in fact not the most efficient way to excite the MDR, as most of the light is coupled to the non-resonating, dissipative modes. Our calculations aim to illustrate the resonant behavior and the corresponding strong optical forces. In actual implementation, other form(s) of incident light wave (e.g. evanescent wave) can be used to realize a stronger force and thereby to utilize the full potential of the resonant effect. We also note that while absorption will degrade the strength of the resonance, microspheres containing gain materials can in principle enhance the resonant force, and the effect should be most interesting when the WGM starts lasing.¹⁰ These would be interesting topics for further studies.

Support by Hong Kong RGC through CA02/03.SC05 and HKUST6138/00P is gratefully acknowledged. Zhifang Lin is also supported by CNKBRFSF and NNSF of China. C.T. Chan’s e-mail address is phchan@ust.hk.

References

1. J. Ng, Z.F. Lin, C.T. Chan and P. Sheng, “Photonic Clusters”, available at <http://arXiv.org/abs/cond-mat/0501733>.
2. M.M. Burns, J-M Fournier and J.A. Golovchenko, *Phys. Rev. Lett.* **63**, 1233 (1989).

3. S.A. Tatarkova, A.E. Carruthers and K. Dholakia, *Phys. Rev. Lett.* **89**, 283901 (2002).
4. H. Xu and M. Kall, *Phys. Rev. Lett.* **89**, 246802 (2002).
5. M.I. Antonoyiannakis and J.B. Pendry, *Europhys. Lett.* **40**, 613 (1997).
6. W. Singer, M. Frick, S. Bernet and M. Ritsch-Marte, *J. Opt. Soc. Am. B* **20**, 1568 (2003).
7. P.C. Chaumet and M. Nieto-Vesperinas, *Phys. Rev. B* **64**, 035422 (2001).
8. T. Mukaiyama, K. Takeda, H. Miyazaki, Y. Jimba and M. Kuwata-Gonokami, *Phys. Rev. Lett.* **82**, 4623 (1999).
9. Y.P. Rakovich, J.F. Donegan, M. Gerlach, A.L. Bradley, T.M. Connolly, J.J. Boland, N. Gaponik and A. Rogach, *Phys. Rev. A* **70**, 051801 (2004).
10. Y. Hara, T. Mukaiyama, K. Takeda and M. Kuwata-Gonokami, *Opt. Lett.* **28**, 2437 (2003).
11. Y.L. Xu, *Appl. Opt.* **34** 4573 (1995).
12. H. Miyazaki and Y. Jimba, *Phys. Rev. B* **62**, 7976 (2000).
13. V. Fraysse, L. Giraud, S. Gratton and J. Langou, CER-FACS Technical Report TR/PA/03/3 (2003).
14. K.A. Fuller, *Appl. Opt.* **30**, 4716 (1991).
15. See e.g., J. Israelachvili, *Intermolecular and Surface Forces*, 2nd ed. (Academic Press, London, 1991).